

**Ministry of Higher Education
and Scientific Research
University of Diyala
College of Engineering**



Design and Fabrication of Miniature Thermoacoustic Cooler for Electric Boards

**A Thesis Submitted to Council of College of Engineering,
University of Diyala in Partial Fulfilment of the
Requirements for the Degree of Master of Science in
Mechanical Engineering**

**By
Oday Shaker Mahmood**

**Supervised by
Prof. Dr. Abdul Mun'em A. Karim
Assist. Prof. Dr. Samir Gh. Yahya**

May, 2021

IRAQ

Ramadan, 1442

Supervisor Certificate

I certify that this thesis entitled (**Design and Fabrication of Miniature Thermoacoustic Cooler for Electric Boards**) had been carried out under my supervision at the University of Diyala/College of Engineering/ Mechanical Engineering Department in partial fulfillment of the requirements for the degree of Master of Science in Mechanical Engineering.

Signature:

Name: **Prof. Abdul Mun'em A. Karim (Ph.D.)**

Date: / / 2021

Signature:

Name: **Asst. Prof. Samir Gh. Yahya (Ph.D.)**

Date: / / 2021

In view of the available recommendation, I forward this thesis for debate by the examination committee.

Signature:

Name: **Asst. Prof. Dhia Ahmed Salal (Ph.D.)**

Head of the Mechanical Engineering Department

Date: / / 2021

Examination Committee Certificate

We certify that we have read this dissertation entitled (**Design and Fabrication of Miniature Thermoacoustic Cooler for Electric Boards**) and as an examining committee examined the student (**Oday Sh. Mahmood**) in its contents and that in our opinion it meets standard of a thesis and is adequate for the award of the degree of Master of Science in Mechanical Engineering.

Signature:

Name: **Prof. Abdul Mun'em A. Karim (Ph.D.)** (Supervisor)

Date: / / 2021

Signature:

Name: **Asst. Prof. Samir Gh. Yahya (Ph.D.)** (Supervisor)

Date: / / 2021

Signature:

Name: **Prof. Jasim Abdulateef (Ph.D.)** (Member)

Date: / / 2021

Signature:

Name: **Prof. Qasim Saleh Mahdi (Ph.D.)** (Member)

Date: / / 2021

Signature:

Name: **Prof. Lutfi Y. Zedan (Ph.D.)** (Chairman)

Date: / / 2021

Approved by the Council of the College of Engineering

Signature:

Name: **Prof. Anees Abdulla Khadom (Ph.D.)**

Dean of the College of Engineering

Date: / / 2021

ACKNOWLEDGEMENT

First and foremost, **praise be to Allah**, by whose grace has this study was fulfilled.

I wish to acknowledgement my great gratitude to the supervisor, **Prof. Dr. Abdul Mun'em A. Karim and Assist. Prof. Dr. Samir Gh. Yahya** who gave me invaluable support throughout the course of the study with their academic experience, patience, understanding and encouragement. Their support has contributed to the development of my skills and confidence in conducting independent and rigorous practical research. Thanks to their supervision and advice, my scientific thesis became interesting despite the difficult circumstances that I faced throughout the research period.

My thanks and appreciation go to the college of engineering, especially the Mechanical Engineering Department, for providing the right place and the requirements of practical experiments.

I extend my thanks and love to my dear mother who supports me with her prayers. She is the source of my inspirations after God. I would like to thank my loved wife for her patience and providing comfort to me, and to my children Rami, Rawan, Amin and Shaker who are my source of encouragement. I thank my brothers Luay, Ali and Mohammed, may God have mercy on him, and my sisters, for their support in completing the research.

I would like to thank the Diyala State Company for their support and assistance in the manufacture of the device, especially the technical department, and the engineer Rabah Sabaa and his staff, and the technical Ali Inad for his instructions regarding the gas system, and for everyone who helped me in my research.

Finally, I present this work to my dear father, who passed away, and I have always hoped that he would be by my side support in my studies.

TABLE OF CONTENTS

| | |
|--|-------------|
| ACKNOWLEDGEMENT | i |
| TABLE OF CONTENTS | ii |
| LIST OF FIGURES | v |
| LIST OF TABLES | ix |
| LIST OF SYMBOLS AND ABBREVIATIONS | x |
| ABSTRACT | xiii |
| CHAPTER ONE INTRODUCTION | 1 |
| 1.1 Thermoacoustics | 1 |
| 1.2 History of Thermoacoustics..... | 1 |
| 1.3 Thermoacoustic Effect..... | 4 |
| 1.4 The Governing Equations | 6 |
| 1.5 Principle of Thermoacoustics | 8 |
| 1.5.1 Wavelength (λ) | 8 |
| 1.5.2 Thermal Penetration Depth (δk)..... | 8 |
| 1.5.3 Viscous Penetration Depth (δv)..... | 9 |
| 1.5.4 Gas Displacement Amplitude | 10 |
| 1.5.5 Relative Pressure Amplitude (RPA) | 12 |
| 1.5.6 Lautrec Number (N_L)..... | 12 |
| 1.5.7 Working Gas | 13 |
| 1.5.8 Mean Pressure (P_m) | 13 |
| 1.5.9 The Frequency (f)..... | 14 |
| 1.6 DeltaEC Software | 14 |
| 1.7 The Motivation behind the Study | 15 |
| 1.8 Objectives of the Present Study | 16 |
| 1.9 Outline of Thesis..... | 18 |
| CHAPTR TWO LITERATURE REVIEW | 19 |
| 2.1 Practical Thermoacoustic Devices..... | 19 |
| 2.1.1 Standing Wave Thermoacoustic Refrigerator | 20 |
| 2.1.2 Travelling Wave Thermoacoustic Refrigerator..... | 26 |

| | |
|---|-----------|
| CHAPTER THREE MODELLING AND OPTIMIZATION | 32 |
| 3.1 Design Consideration..... | 32 |
| 3.2 Acoustic Driver/Ordinary Loudspeaker Performance | 32 |
| 3.2.1 Driver’s Performance at Different Acoustic Impedance | 37 |
| 3.2.2 Driver’s Performance at Different Frequency | 40 |
| 3.2.3 Driver’s Performance at Different Peak-to-Peak Displacement | 43 |
| 3.3 Design and Optimization | 46 |
| 3.3.1 The Effect of Diameter and Length Inertance (Neck)..... | 47 |
| 3.3.2 The Effect of Diameter and Length of Looped Tube | 50 |
| 3.3.3 The Effect of Diameter and Length of Regenerator | 53 |
| 3.3.4 The Effect of Length and Volumetric Porosity of Regenerator | 56 |
| 3.3.5 The Effect of Length and Hydraulic Radius of Regenerator..... | 58 |
| 3.3.6 The Effect of Length and Porosity of Heat Exchanger | 61 |
| 3.3.7 The Effect of Length and Hydraulic Radius of Heat Exchanger | 64 |
| 3.4 Final Design (DeltaEC Simulation)..... | 67 |
| CHAPTER FOUR EXPERIMENTAL APPARATUS..... | 72 |
| 4.1 Description of Components of Thermoacoustic Cooler | 72 |
| 4.2 Main Components: Descriptions and Details | 73 |
| 4.2.1 Heat Exchangers | 73 |
| 4.2.2 The Regenerator..... | 75 |
| 4.2.3 Other Components | 76 |
| 4.2.4 The Acoustic Driver Housing | 77 |
| 4.3 Instrumentation | 78 |
| CHAPTER FIVE RESULTS AND DISCUSSION | 80 |
| 5.1 No-Load Experiments | 80 |
| 5.1.1 Effect of the Operating Frequency | 80 |
| 5.1.2 Effect of the Mean Pressure..... | 82 |
| 5.2 Active Load experiments | 84 |
| CHAPTER SIX CONCLUSIONS AND RECOMMENDATIONS | 87 |
| 6.1 Conclusions..... | 87 |
| 6.2 Recommendations..... | 88 |
| REFERENCES..... | 90 |

APPENDIX A THE FINAL OPTIMIZED DELTAEC SIMULATION

APPENDIX B THE EXPERIMENTAL APPARATUS WITH FULL DIMENSIONS

B.1 Part Number One

B.2 Part Number Two

B.3 Part Number Three

B.4 Part Number Four

B.5 Part Number Five

B.6 Part Number Six

B.7 Part Number Seven

B.8 Part Number Eight

B.9 Part Number Nine

B.10 Part Number Ten

B.11 Part Number Eleven

B.12 Part Number Twelve

B.13 Part Number Thirteen

APPENDIX C PUBLICATIONS

LIST OF FIGURES

| | |
|---|----|
| Figure 1.1: Higgins’ singing flame (Putnam & Dennis, 1956). | 2 |
| Figure 1.2: Sondhauss tube (Sondhauss, 1850). | 2 |
| Figure 1.3: Rijke tube (Rijke, 1859). | 3 |
| Figure 1.4: Schematic of a simple thermoacoustic refrigerator (a). The heat transfer process by thermoacoustic oscillations in the stack (b) (Mohd Saat & Jaworski, 2017). | 5 |
| Figure 1.5: The gas displacement amplitude variation (Swift, 2001). | 11 |
| Figure 1.6: Heat transfer when gas parcel moves along the heat exchanger and stack, when the length of the heat exchanger is equal to $2\xi_1$ (a), shorter than $2\xi_1$ (b), and longer than $2\xi_1$ (c) (Saechan, 2014). | 12 |
| Figure 2.1: The basic components of thermoacoustic device (Samir et al., 2016). | 19 |
| Figure 2.2: Schematic of standing wave (a) and travelling wave thermoacoustic refrigerator (b) (Tartibu, 2018). | 20 |
| Figure 2.3: Schematic of standing wave thermoacoustic refrigerator (Marx et al., 2006). | 21 |
| Figure 2.4: Schematic of a standing wave refrigerator with 10W cooling power and temperature gradient of 80K (Prashantha et al., 2017). | 22 |
| Figure 2.5: Schematic of experimental setup of the refrigerator (Kamsanam, 2018). | 23 |
| Figure 2.6: Comparison of a temperature difference produced for two stack positions (Harikumar et al., 2019). | 24 |
| Figure 2.7: Schematic and photo of a standing wave thermoacoustic refrigerator (Abd El-Rahman et al., 2020). | 25 |
| Figure 2.8: Schematic of a travelling wave thermoacoustic refrigerator driven by ordinary loudspeaker. | 27 |
| Figure 2.9: Schematic of the refrigerator of experimental setup (Setiawan et al., 2017). | 28 |
| Figure 2.10: The diagram of (r_h/δ_k) versus the maximum temperature decrease $(\Delta T_{C, \max})$ (Setiawan et al., 2017). | 29 |
| Figure 2.11: Schematic of travelling wave thermoacoustic refrigerator (a), COP as a function of the temperature of the hot heat exchanger for different regenerators (b) (Ben Nasr et al., 2018). | 30 |
| Figure 2.12: Schematic of the coupled system, symbols denote: BS - bounce space, HHX - hot heat exchanger, STK - stack, AHX _{SWTE} - ambient heat exchanger (engine), TBT - thermal buffer tube, CHX - cold heat exchanger, | |

| | |
|--|----|
| REG - regenerator, AHX _{TWTC} - ambient heat exchanger (cooler) (a), photograph of the laboratory test rig with instrumentation (b) (Saechan & Jaworski, 2019). | 31 |
| Figure 3.1: The two types of acoustic drivers: ordinary loudspeakers (a), and linear alternators (b). | 33 |
| Figure 3.2: Driver's current (a) and voltage (b) with different acoustic impedance..... | 38 |
| Figure 3.3: Acoustic power (a) and driver's efficiency (b) with different acoustic impedance. | 39 |
| Figure 3.4: driver's current (a) and voltage (b) with different frequencies.... | 41 |
| Figure 3.5: Acoustic power (a) and driver's efficiency (b) with difference frequencies. | 42 |
| Figure 3.6: driver's current (a) and voltage (b) with different peak-to-peak displacement..... | 44 |
| Figure 3.7: Acoustic power (a) and driver's efficiency (b) with peak-to-peak displacement..... | 45 |
| Figure 3.8: Schematic drawing of miniature travelling wave thermoacoustic cooler with an acoustic driver. | 46 |
| Figure 3.9: The effect of diameter and length of inertance on the acoustic impedance (a) and its phase (b)..... | 48 |
| Figure 3.10: The effect of diameter and length of inertance on cooling power (a) and COP (b). | 49 |
| Figure 3.11: The effect of diameter and length of loop tube on the acoustic impedance (a) and its phase (b)..... | 51 |
| Figure 3.12: The effect diameter and length of loop tube on cooling power (a) and COP (b)..... | 52 |
| Figure 3.13: The effect of diameter and length of regenerator on the acoustic impedance (a) and its phase (b)..... | 54 |
| Figure 3.14: The effect diameter and length of regenerator on cooling power (a) and COP (b). | 55 |
| Figure 3.15: The effect of length and volumetric porosity of regenerator on the acoustic impedance (a) and its phase (b). | 57 |
| Figure 3.16: The effect of length and volumetric porosity of regenerator on cooling power (a) and COP (b). | 58 |
| Figure 3.17: The effect of length and hydraulic radius of regenerator on the acoustic impedance (a) and its phase (b). | 59 |
| Figure 3.18: The effect of length and hydraulic radius of regenerator on cooling power (a) and COP (b). | 60 |

| | |
|--|----|
| Figure 3.19: The effect of length and porosity of heat exchanger on the acoustic impedance (a) and its phase (b). | 62 |
| Figure 3.20: The effect of length and porosity of heat exchanger on cooling power (a) and COP (b). | 63 |
| Figure 3.21: The effect of length and hydraulic radius of heat exchanger on the acoustic impedance (a) and its phase (b). | 65 |
| Figure 3.22: The effect of length and hydraulic radius of heat exchanger on cooling power (a) and COP (b). | 66 |
| Figure 3.23: The effect of diameter of inertance on the driver's efficiency (a) and COP (b) of the optimized design of apparatus. | 68 |
| Figure 3.24: The effect of length of inertance on the driver's efficiency (a) and COP (b) of the optimized design of apparatus. | 69 |
| Figure 3.25: The effect of length of loop tube on the driver's efficiency (a) and COP (b) of the optimized design of apparatus. | 70 |
| Figure 3.26: The effect of diameter of loop tube on the driver's efficiency (a) and COP (b) of the optimized design apparatus. | 70 |
| Figure 3.27: The effect of diameter of core on the driver's efficiency (a) and COP (b) of the optimized design of apparatus. | 70 |
| Figure 3.28: The effect of hydraulic radius of heat exchanger on the driver's efficiency (a) and COP (b) of the optimized design of apparatus. | 71 |
| Figure 4.1: A cross-section of thermoacoustic cooler: 1- Acoustic driver housing, 2- Acoustic driver, 3- Reducer, 4- Neck pipe, 5- Expander, 6- Looped tube, 7- AHX, 8- Regenerator and 9- CHX. | 73 |
| Figure 4.2: An actual photo of the used ambient heat exchanger (AHX). | 74 |
| Figure 4.3: An actual photo of the used cold heat exchanger (CHX). | 75 |
| Figure 4.4: An actual photo of the regenerator and the woven mesh screens/discs. | 76 |
| Figure 4.5: An assembly drawing of the cooler structure. | 77 |
| Figure 4.6: Schematic and Photograph of actual thermoacoustic cooler and the used instrumentation when set in the laboratory. | 79 |
| Figure 5.1: The effect of experimental operating frequency on the temperature difference at the ends of regenerator. | 81 |
| Figure 5.2: Distribution of the experimentally measured and simulation temperature along the regenerator. | 82 |
| Figure 5.3: The effect of mean pressure on the experimentally-measured temperature difference at the ends of regenerator. | 83 |
| Figure 5.4: Distribution of the experimentally measured and simulation temperatures along the regenerator at different mean pressure. | 84 |

| | |
|---|----|
| Figure 5.5: The effect of cooling power on the temperature difference at the ends of regenerator..... | 85 |
| Figure 5.6: Distribution of the experimentally measured and simulation temperature along the regenerator at cooling power..... | 86 |

- Figure B. 1:** Parts numbering of the experimental apparatus.
- Figure B. 2:** Two-dimensional drawing of the acoustic driver housing.
- Figure B. 3:** Two-dimensional drawing of the reducer.
- Figure B. 4:** Two-dimensional drawing of the inertance.
- Figure B. 5:** Two-dimensional drawing of the expander.
- Figure B. 6:** Two-dimensional drawing of the triple pipe.
- Figure B. 7:** Two-dimensional drawing of the looped tube -1.
- Figure B. 8:** Two-dimensional drawing of the elbow.
- Figure B. 9:** Two-dimensional drawing of the looped tube-2.
- Figure B. 10:** Two-dimensional drawing of the expander of core.
- Figure B. 11:** Two-dimensional drawing of the ambient heat exchanger.
- Figure B. 12:** Two-dimensional drawing of the holder of regenerator.
- Figure B. 13:** Two-dimensional drawing of the cold heat exchanger.
- Figure B. 14:** Two-dimensional drawing of the reducer of core.

LIST OF TABLES

| | |
|--|----|
| Table 3.1: The main specification of loudspeaker. | 34 |
| Table 3.2: The final optimum dimensions and details of the components cooler. | 67 |
| Table 3.3: Dimensions and details of the actual design of thermoacoustic cooler. | 71 |
| Table 4.1: The locations of thermocouple along the regenerator | 78 |

LIST OF SYMBOLS AND ABBREVIATIONS

| | |
|-----------|---|
| A | Cross- section area, m^2 |
| a | Speed of sound, m/s |
| C | Compliance of acoustic networks, m^3/pa |
| C_p | Isobaric specific heat capacity, J/kg.K |
| E | Energy, W |
| \dot{E} | Acoustic power, W |
| f | Frequency, Hz |
| I | Current, Amps |
| i | $\sqrt{-1}$ |
| K | Spring constant, N.t/m |
| k | Thermal conductivity, W/m.K |
| L | Inertance of acoustic networks, kg/m^4 |
| l | Length, m |
| M | Mass, kg |
| N_L | Lautrec number |
| P | Pressure, Pa |
| Q | Heat, J; Thermal power, W |
| R_e | Electrical resistance, Ohm |
| R_m | Mechanical resistance, kg/s |
| r_h | Hydraulic radius, m |
| T | Temperature, K, °C |
| t | Time, s |
| U | Volumetric flow rate , m^3/s |
| u | Velocity in x direction, m/s |
| V | Volume, m^3 |

| | |
|----------------|---|
| V | Voltage, V |
| W | Work done, W |
| 2Y | Spacing of Parallel plate stack, m |
| Z _a | Acoustic impedance, Pa.s/m ³ |

Greek Letters

| | |
|---|--|
| Δ | Difference |
| γ | Ratio of isobaric to isochoric specific heats |
| δ | Penetration depth, m |
| ξ | Peak-to-peak displacement of driver's diaphragm, m |
| θ | Phase angle, degree |
| λ | Wave-length, m |
| μ | Dynamic viscosity, kg/m.s |
| ρ | Density, kg/m ³ |
| σ | Prandtl number |
| ω | Angular frequency, s ⁻¹ |

Subscripts

| | |
|-----|----------------------------|
| A.D | Acoustic driver |
| C | Compliance |
| c | Cooling load |
| E | Engine |
| e | Electric |
| H | High temperature |
| I | Current |
| k | Thermal |
| L | Inertance, low temperature |
| m | Mean value |

| | |
|-------|--|
| p | Pressure |
| R | Refrigerator |
| U | Volume flow rate |
| V | Voltage |
| Z_a | Acoustic impedance |
| 1 | First order of acoustic variables, usually a complex amplitude |
| 2 | Second order of acoustic variables |
| in | Inlet |
| out | Outlet |
| v | Viscous |

Special Symbols

| | |
|------------|-----------------------------|
| $R_c []$ | Real part of |
| $ $ | Magnitude of complex number |
| ∂ | Partial derivative |

Abbreviations

| | |
|---------|--|
| AHX | Ambient heat exchanger |
| BL | Force factor |
| CHX | Cold heat exchanger |
| COP | Coefficient of performance |
| COP_C | Carnot coefficient of performance |
| COP_R | Coefficient of performance relative to Carnot |
| DC | Direct current |
| DeltaEC | Design Environment for Low-amplitude Thermoacoustic Energy |
| HHX | Hot heat exchanger |

ABSTRACT

The current research focuses on the design and fabrication of an efficient miniature thermoacoustic cooler capable of producing sufficient cooling power to cool electric boards.

In theory, it was aimed that the thermoacoustic cooler was assigned to achieve 30 - 50 W of cooling power at a temperature difference of 25°C between the cold and the ambient sides.

The first part of the research deals with how the loudspeaker is coupled with a travelling wave thermoacoustic cooler. This includes analyzing the equations that govern the dynamic behavior of the loudspeaker, which leads to achieving the appropriate acoustic conditions for the optimum performance of the cooler. A series of DeltaEC simulations were performed to verify the possible acoustic network configurations to meet the required acoustic conditions of the used ordinary loudspeaker.

As for the second part, it deals with the geometry of the experimental apparatus. The fabricated travelling-wave thermoacoustic cooler operates by frequency of 95Hz (practically optimal) and uses helium gas at 1bar of gauge pressure. The experimental apparatus achieved a maximum temperature difference of 5.7°C (between the ambient/hot and cold ends when no cooling load was applied) and 1°C (at maximum cooling power of 37W).

CHAPTER ONE

CHAPTER ONE

INTRODUCTION

In this chapter, the concepts and fundamentals of Thermoacoustics will be reviewed along with the governing equations and some selected important parameters.

1.1 Thermoacoustics

Nicholas Rott (Rott, 1980), who was the first to introduce the term Thermoacoustics which laid to establishing the theoretical foundations of this phenomenon. Thermoacoustics is the science name to describe a thermoacoustic effect that defines the conversion from the acoustics to thermal powers and vice versa. In other words, it is an interaction between the heat and soundwaves to achieve either cooling power (refrigeration) or electricity (prime movers). To achieve the conversion from the thermal power into an acoustic power a thermoacoustic engine is required, while the reverse process can be achieved via a thermoacoustic refrigerator.

1.2 History of Thermoacoustics

The history of Thermoacoustics dates back to several centuries. The first to report the phenomenon of thermoacoustic effect was Bryan Higgins in 1802 (Graiff, 1964). Higgins proved in 1777 that burning an amount of hydrogen near the opening of a vertical glass tube produces a sound (Putnam & Dennis, 1956), which is called “singing flame” (see Figure 1.1). Higgins noted that the sound generated in the tube depends on the location and intensity of the flame as well as the length and diameter of the tube.

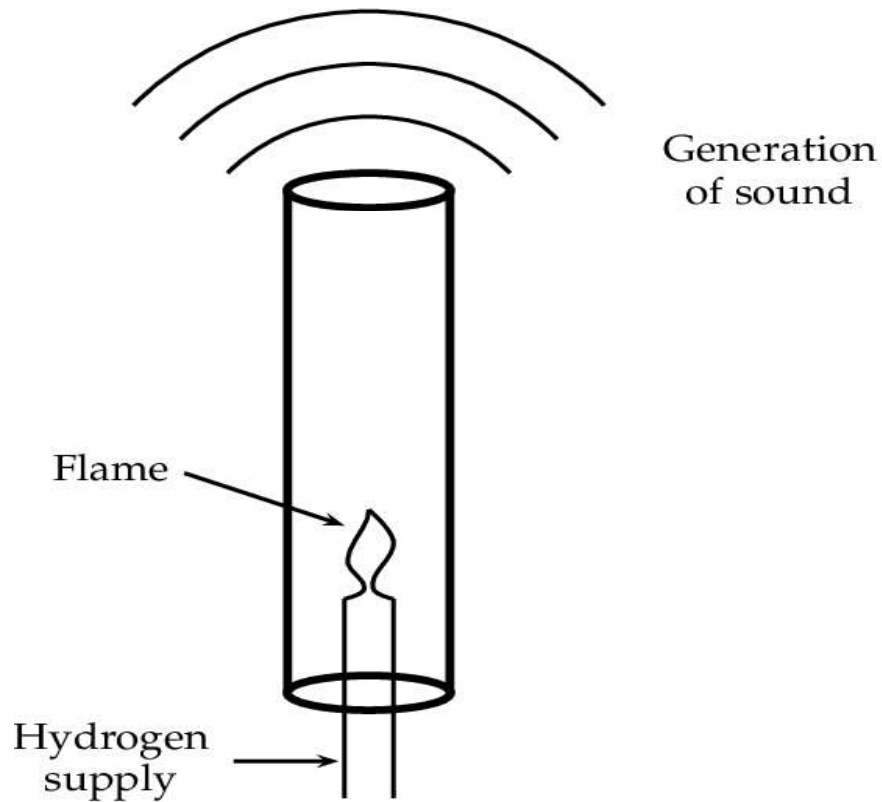


Figure 1.1: Higgins' singing flame (Putnam & Dennis, 1956).

(Sondhauss, 1850) performed different experiment using an open-closed tube (see Figure 1.2). A flame was placed on the bulb at the closed end producing in a sound at the open end. Sondhauss indicated that the oscillation of sound depends on the size of the bulb and the intensity of the flame, and the sound increases at more heated.

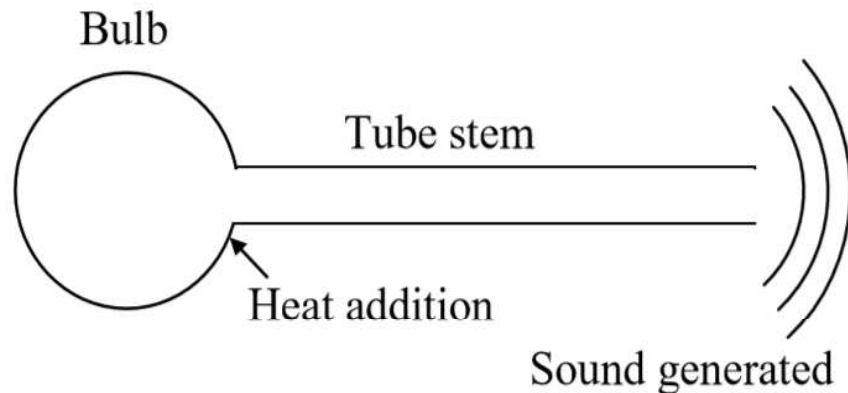


Figure 1.2: Sondhauss tube (Sondhauss, 1850).

(Rijke, 1859) investigated the acoustic oscillations in a similar apparatus while replacing the flame with a mesh of heated wire (see Figure 1.3), Rijke found that sound is produced only when the tube is perpendicular and the heated mesh is fixed to the bottom of tube, and indicated that the convection flow produced from heating the air in the tube is important in the generation of acoustic oscillation.

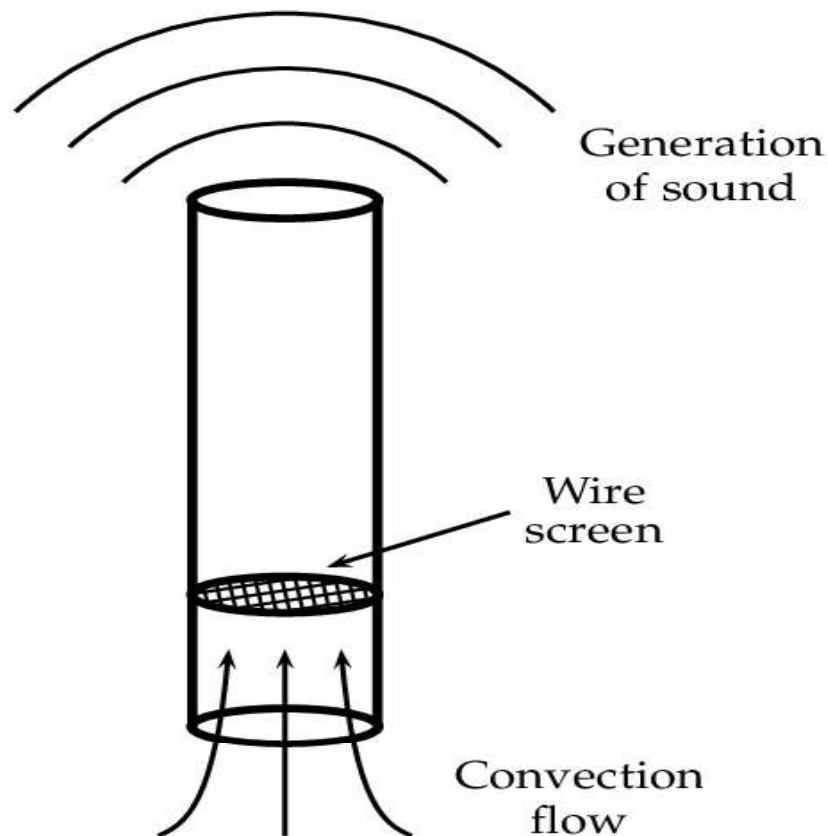


Figure 1.3: Rijke tube (Rijke, 1859).

(Taconis et al., 1949) observed another form of Sondhauss vibration by dealing with liquid helium in a glass tube. A large temperature gradient was imposed between the temperature of tube and surrounding causing sound oscillations inside the tube.

In 1969, a major breakthrough occurred with Rott investigations into Thermoacoustics, Rott managed to develop his theory of designing

thermoacoustic devices (refrigerators and engines). An investigation was beginning at Los Alamos National Laboratory (LANL) in the early 1980s. Hofler and Swift (Hofler, 1986, Swift, 1997) were among those most interested in largely developing thermoacoustic devices. The first to design and build a fully functioning thermoacoustic refrigerator is Hofler in 1986. Later, a lot of studies and research have emerged that contributed significantly to development of thermoacoustic devices, and to this day, this study is an extension of them.

1.3 Thermoacoustic Effect

Acoustic waves are pressure oscillations in the space that can create temperature fluctuations associated with the compression and expansion of the pressure waves (Garrett & Backhaus, 2000). One method of extracting useful work from acoustic waves is to place a solid with high specific heat capacity and a large surface area in contact with oscillating gas. Due to the higher specific heat capacity of the solid compared to gas, the solid can store heat and exchange it with gas. When the volume of gas expands in the oscillation cycle, the gas cools and absorbs heat from the solid, while rejecting heat to the solid when gas compressed as it becomes hot. The working principle of Thermoacoustics is illustrated by the following example (see Figure 1.4) by taking a long tube filled with gas, this tube includes a solid metal with a high specific heat capacity and a low thermal conductivity known as the stack (random or regular porous medium). The geometry of the stack is characterized by containing pores for the acoustic waves to travel through it.

To create the thermoacoustic effect requires a large temperature gradient across the ends of the stack by placing two heat exchangers in contact with the ends, one at low temperature (cold heat exchanger) and the other at high temperature (hot heat exchanger).

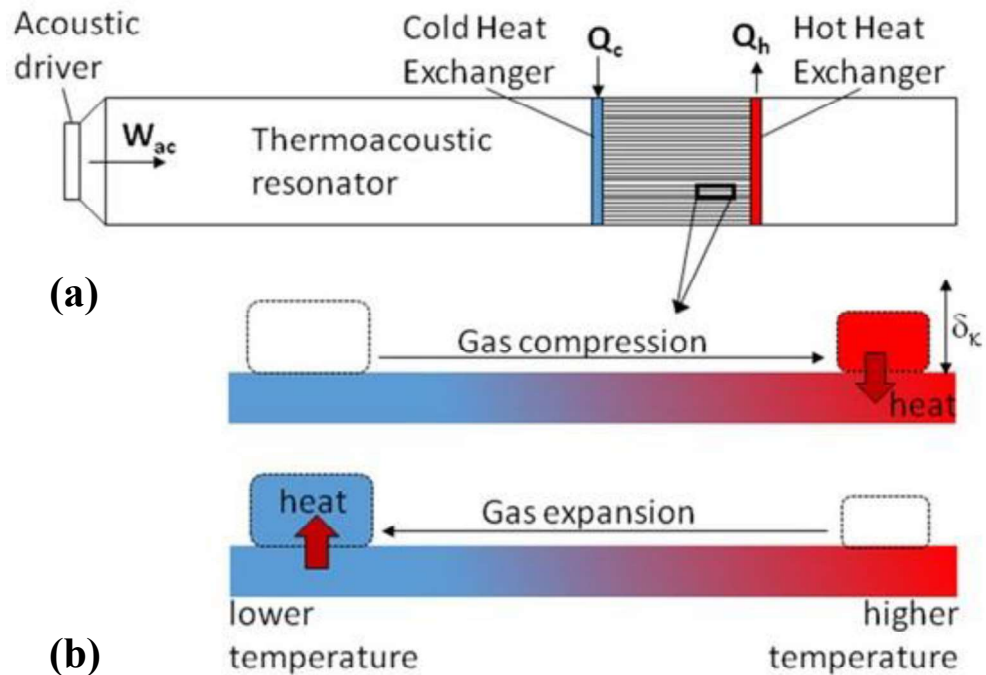


Figure 1.4: Schematic of a simple thermoacoustic refrigerator (a). The heat transfer process by thermoacoustic oscillations in the stack (b) (Mohd Saat & Jaworski, 2017).

Here, an acoustic driver can be used to generate the necessary oscillating acoustic power/wave moving back and forth inside the tube (see Figure 1.4). The gas will be compressed during its movement towards the hot heat exchanger (velocity node) and its temperature will increase to become higher than the temperature of the stack's metal (hot heat exchanger side), which leads to heat transfer to the solid. When the gas moves towards the cold heat exchanger (pressure node) it will be expanded and become colder than the metal of the stack and heat will be transferred to the gas. The process of gas absorption of heat from a solid metal with a low temperature and conversion heat to another solid with high temperature is thermoacoustic refrigeration (thermoacoustic effect).

The difference in gas temperature at both the ends of the stack is due to the adiabatic compression and expansion of the gas. The perpendicular distance to the direction of propagation of the acoustic wave mainly effects the heat transfer

is known as the thermal penetration depth (δ_k). This distance depends on the frequency of the acoustic wave and the properties of the gas, which will be explained later. For the finest heat transfer between the gas and solid, the recommended spacing between one plate and another of the stack through the gas passes should be about twice as the thermal penetration depth (Swift, 2001).

1.4 The Governing Equations

For one-dimensional acoustic wave oscillating at an angular frequency $\omega=2\pi f$, where (f) is the frequency of oscillation, the governing equations of such wave can be expressed with the dependence of the typical quantities of pressure, velocity, temperature, density and entropy considered in Thermoacoustics and according to the following equations (Swift, 2001):

$$P(x, y, z, t) = P_m + R_e [P_1(x) e^{i\omega t}] \quad 1.1$$

$$u(x, y, z, t) = R_e [u_1(x, y, z) e^{i\omega t}] \quad 1.2$$

$$T(x, y, z, t) = T_m(x) + R_e [T_1(x, y, z) e^{i\omega t}] \quad 1.3$$

$$\rho(x, y, z, t) = \rho_m(x) + R_e [\rho_1(x, y, z) e^{i\omega t}] \quad 1.4$$

$$S(x, y, z, t) = S_m(x) + R_e [S_1(x, y, z) e^{i\omega t}] \quad 1.5$$

Where:

(x) is the distance along the direction of penetration of the acoustic wave.
 (y) is the direction perpendicular to the direction of penetration.
 (z) is the direction perpendicular to the plane of the paper in depth.
 The number (1) denotes first order expansion of the complex terms. (m) denotes the mean value of the variable. The term ($e^{i\omega t}$) represents the oscillating portion associated with the acoustic wave.

The above equations depend on some assumptions (Swift, 2001). For example, the dependence of oscillating pressure in the direction of (x) and its neglected

in the direction (y & z), the mean velocity is assumed to be zero (no mean flow) because the flow in the system is uniform and independent in all directions.

Equations (1.1) to (1.5) are derived from the three basic equations which are the continuity, momentum and heat transfer equations. Here some assumptions were considered as follow: the propagation of the acoustic wave in the direction of (x) only, steady oscillating flow with the terms of the second order being neglected (Swift, 2001):

- Continuity equation:

$$i\omega\rho_1 + \frac{d\rho_m}{dx}u_1 + \rho_m \nabla \cdot v_1 = 0 \quad 1.6$$

- Momentum equation:

$$i\omega\rho_m u_1 = -\frac{dp_1}{dx} + \mu \left(\frac{\partial^2 u_1}{\partial y^2} + \frac{\partial^2 u_1}{\partial z^2} \right) \quad 1.7$$

- Heat transfer equation:

$$i\omega\rho_m C_P T_1 + \rho_m C_P \frac{dT_m}{dx} u_1 = i\omega p_1 + k \left(\frac{\partial^2 T_1}{\partial y^2} + \frac{\partial^2 T_1}{\partial z^2} \right) \quad 1.8$$

In general, any thermoacoustic system includes a network of channels/pipes consisting of compliance, inertance and resistance are necessary to produce a near traveling-wave phasing within the regenerator, where the compliance in the acoustic networks similar to the capacitance in an electric network, while the inertance in similar to the inductance in an electric network (Swift, 2001).

The gas compressibility $\left(\frac{1}{\gamma p_m}\right)$ with a short channel volume (V), or compliance (C) is as follows:

$$C = \frac{V}{\gamma p_m} \quad 1.9$$

Where (γ) is the specific heat ratio, (p_m) is the mean pressure.

Similarly, the inertial properties of the gas within a long channel, or inertance is as follows:

$$L = \frac{\rho_m \Delta x}{A} \quad 1.10$$

Where (ρ_m) is the density of the gas, (Δx) and (A) are the length and cross-sectional area of the channel respectively.

The acoustic characteristics combine to form the acoustic impedance (Z_a), which is the ratio of pressure to volume flow rate ($Z_a = \frac{p_1}{U_1}$), the acoustic impedance describes the resistance of thermoacoustic system network to the working gas.

1.5 Principle of Thermoacoustics

In this section, the important parameters used in the design and operation of thermoacoustic devices will be presented and described (Swift, 2001).

1.5.1 Wavelength (λ)

When an acoustic wave is propagated in a gas, it must have length which known as the wavelength and has a great effect on the length of thermoacoustic devices and the energy density of the system, usually the thermoacoustic device has a length less than the wavelength, it can be calculated by the following equation:

$$\lambda = \frac{a}{f} \quad 1.11$$

Where (a) is the speed of the sound.

1.5.2 Thermal Penetration Depth (δ_k)

Thermal penetration depth is an important parameter which gives an idea about heat diffusion according to the distance between the gas and solid surface of the stack or regenerator. In other words, it is the thickness of the layer surrounding

the stack's plate or regenerator through which the heat transfer takes place. This depth is perpendicular to the direction of propagated acoustic wave and can be calculated by the following equation:

$$\delta_k = \sqrt{\frac{2k}{\omega\rho C_p}} \quad 1.12$$

Where (k), (ρ) and (C_p) are the thermal conductivity, the density and the specific heat of the gas respectively.

1.5.3 Viscous Penetration Depth (δ_v)

This depth is the thickness of the layer around the stack or regenerator which shows the important viscous effects, as the viscous shear forces occur within this layer and lead to the dissipation of the acoustic power, it can be expressed by the following equation:

$$\delta_v = \sqrt{\frac{2\mu}{\omega\rho}} \quad 1.13$$

Where (μ) is the dynamic viscosity.

The viscous penetration depth is one of the important parameters to determine the optimum spacing between the plates of stack or regenerator, the distance between these plates should be less than the thermal penetration depth. As an illustrative example, the gas does not feel any thermal and viscous contact when moves through the plates because the distance between the solid boundaries is much greater than the thermal and viscous penetration depth (Swift, 2001). It must be noted that there is a trade-off between thermal and viscous penetration depth, the Prandtl number (σ) determines the ratio of the differentiation between two penetration depths by the following equation:

$$\sigma = \left(\frac{\delta_v}{\delta_K} \right)^2 = \frac{\mu C_p}{k} \lesssim 1 \quad 1.14$$

To reduce the effect of viscous shear forces the Prandtl number should be less than one (Swift, 2001).

1.5.4 Gas Displacement Amplitude ($|\xi_1|$)

It is an important length scale in the direction of propagation of the acoustic wave, calculated by the following equation:

$$|\xi_1| = \frac{|U_1|}{\omega A} \quad 1.15$$

Where ($|U_1|$) is the volume flow rate amplitude.

The gas displacement represents half of the total tour of the gas during one acoustic cycle. The maximum displacement amplitude of the gas ($2|\xi_1|$) represents back and forth from the peak-to-peak for each acoustic oscillation cycle (Abduljalil et al., 2012; Swift, 2001). In thermoacoustic engines and refrigerators, the gas displacement amplitude is much greater than the penetration depths but much less than the acoustic wavelength (Swift, 2001), as shown in the following equation:

$$\delta_v, \delta_k \ll |\xi_1| \ll \lambda \quad 1.16$$

The displacement amplitude of the gas is very small fraction when compared to the length of tube that is equal to the half or quarter wavelength for standing wave devices. It can be seen that the maximum displacement is larger in the medium and decreases towards the velocity node, as shown in the Figure 1.5.

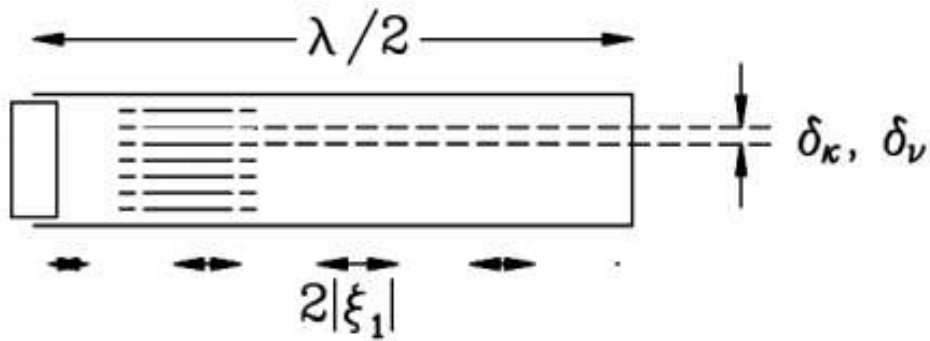


Figure 1.5: The gas displacement amplitude variation (Swift, 2001).

The displacement amplitude can be used to determine the length of the heat exchanger in thermoacoustic devices. The length of the heat exchanger, which equals to the maximum displacement amplitude ($2|\xi_1|$), ensures that most of the heat is transferred to and from the stack or regenerator plate when the gas moves back and forth within the maximum displacement amplitude ($2|\xi_1|$) from the peak-to-peak see Figure 1.6(a), the amount of the heat transferred will decrease when the length of heat exchanger is less than the maximum displacement amplitude ($2|\xi_1|$) because part of the gas parcel will lose their heat outside the heat exchanger as shown in Figure 1.6(b). Finally, if the length of the heat exchanger is greater than the maximum displacement amplitude ($2|\xi_1|$), then all the gas parcel will move along the heat exchanger only, thus it cannot transfer heat to and from the stack or regenerator plate as shown in Figure 1.6(c) (Saechan, 2014).

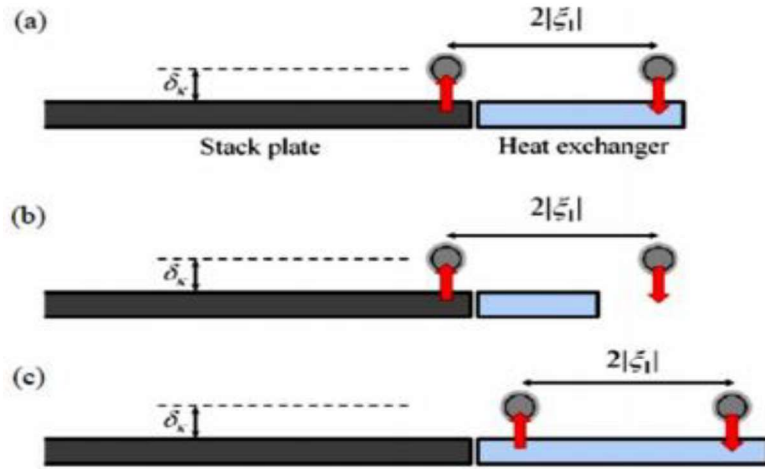


Figure 1.6: Heat transfer when gas parcel moves along the heat exchanger and stack, when the length of the heat exchanger is equal to $2|\xi_1|$ (a), shorter than $2|\xi_1|$ (b), and longer than $2|\xi_1|$ (c) (Saechan, 2014).

Therefore, the ideal length of the heat exchanger is equal to the maximum displacement amplitude of the gas.

1.5.5 Relative Pressure Amplitude (*RPA*)

It is the ratio of pressure amplitude ($|P_1|$) to the mean pressure (P_m) and expressed it according to the following equation:

$$RPA = \frac{|P_1|}{P_m} * 100\% \quad 1.17$$

Relative pressure amplitude also known as the drive ratio is an important parameter for determining the strength of thermoacoustic oscillation which effects the intensity of the acoustic power.

1.5.6 Lautrec Number (N_L)

The Lautrec number can be used to distinguish between stacks and regenerators. If the Lautrec number is greater or equal to one, then the porous medium is called the stack, while the porous medium is called the regenerator if Lautrec number is less than one (Garrett, 2004), which is the ratio of hydraulic radius of

stack or regenerator (r_h) to the depth of thermal penetration and expressed it according the following equation:.

$$N_L = \frac{r_h}{\delta_k} \quad 1.18$$

1.5.7 Working Gas

The working gas plays an important role in thermoacoustic applications with many considerations such as, power, efficiency, etc. The ideal properties of the gas that used in thermoacoustic devices are the Prandtl number (should be less than one as mentioned earlier), high thermal conductivity that increases the gas's ability to transfer the heat between the stack walls and heat exchanger, low viscosity to avoid the viscous shear forces causing the dissipation of the acoustic power (Swift, 2001). In addition, Swift has noted that the higher speed of sound can produce higher power. Inert gases such as, air, nitrogen, helium, neon and other are suitable for use in thermoacoustic devices because they are characterized by low Prandtl number, high sound speed, high thermal conductivity, low viscosity and being environmentally friendly. Helium gas is used more frequently in thermoacoustic devices for its best properties among the inert gases. Therefore, helium will be used in this project as a working gas for the current miniature thermoacoustic cooler.

1.5.8 Mean Pressure (P_m)

The power density is directly proportional to the mean pressure ($\dot{E}_2 \propto P_m$) in the thermoacoustic system (Ceperley, 1979), the acoustic power increase with the increase of the mean pressure. However, higher mean pressure (few bars higher than the atmospheric pressure) can lead to quite complicated design due to the requirements of special design of high pressure vessels in addition to the higher cost. It is important to note that the thermal penetration depth is inversely proportional to the square root of the mean pressure ($\delta_k \propto \frac{1}{\sqrt{p_m}}$), the high mean

pressure results in building a small flow channel size in the regenerator, which makes it difficult and more expensive (Z. Yu et al., 2010).

1.5.9 The Frequency (f)

The power density in thermoacoustic devices is proportional to the frequency ($\dot{E}_2 \propto f$) (Z. Yu & Al-Kayiem, 2014), while the thermal penetration depth is inversely proportional to the frequency ($\delta_k \propto \frac{1}{f}$). The cost of building the regenerator can be increased as high operating frequency being used to operate thermoacoustic devices (Putnam & Dennis, 1956).

1.6 DeltaEC Software

DeltaEC is a computer program/software that used to provide an estimation of how thermoacoustic systems perform and it's the abbreviation of (Design Environment for Low-amplitude Thermo Acoustic Energy Conversion). The program was previously written by Bill Ward and Gregory Swift of Los Alamos National Laboratory (LANL).

The DeltaEC program is numerical tools to solve/integrate the continuity, momentum and energy equations for thermoacoustic devices. DeltaEC is based on the linear thermoacoustic theory which means that all variables oscillate in one direction (x-direction). The program uses a simplified one-dimensional approximation and consider that the amplitude oscillation is low and has a sinusoidal time dependence. The model include a number of segments assembled together by the user that reflect the physical properties of the thermoacoustic devices and assume one-dimensional problem throughout the segment. It assumes that all oscillating variables have a time dependence on $\text{Re}(e^{i\omega t})$. This assumption transforms the governing equations from differential equations in time to algebraic equations for time, making them much easier to solve than the initial partial differential equations (Chinn et al., 2011).

The program integrates the one-dimensional wave equation numerically to obtain a convergent solution through the use of an iterative shooting process. The shooting process begins with a guess value of model parameters and then being integrated through the model. After each round of integration, DeltaEC compares the target values (output) with the guess values (input). If the targets do not match, the guesses are adjusted and the integral is repeated. If the difference between guess and target is equal to zero, then this leads to a convergent solution (target is met) and vice versa (Mitchell, 2012).

Essentially, the user can build a thermoacoustic system by selecting the required acoustic elements as needed. DeltaEC program gives a high flexibility to choose different thermoacoustic system segments, such as volume and shape of compliance and inertance channels, heat exchanger type, regenerator, etc. After the system is fully built, DeltaEC begins solving the appropriate one-dimensional wave equation through each of these segments. The program does this by ensuring that the pressure and volume flow rate are matched at the boundaries of each segment (Telesz, 2006).

1.7 The Motivation behind the Study

There are several reasons that motivated the study, design and development of a thermoacoustic cooler.

- unlike the traditional refrigerators (vapor compression refrigerators), thermoacoustic coolers have no moving mechanical parts which can lead to more reliability, low maintenance and a much longer operating life.
- Traditional refrigerators use highly effective gases that deplete the ozone layer and cause environmental pollution, and despite the use of alternative gases that do not harm the environment such as propane and butane, they are highly flammable gases that pose a great danger if a leak

occurs in the system of these refrigerators. Hence, this has motivated many of the researchers to find an alternative cooling system that is safer and less harmful to the environment. Thermoacoustic refrigerators are the very strong candidate to accomplish this. They are safe and environmentally friendly because the use of inert gases as working gas in their systems. Inert gases has the advantages of being low chemical effectiveness as well as non-flammable and non-toxic.

- Thermoacoustic systems has the advantage of using different sources of energy (as the input work), including the solar, biomass and waste thermal energies (Shen et al., 2009).

Although the advantages of thermoacoustic devices in the mechanical simplicity, low cost, environmental and personal safety, they are still unable to compete with the vapor compression refrigerators due to their low production of cooling powers and relatively low efficiency as being a new technology in the process of research. This technology is supposed to go through the stages of development as those previously passed by traditional devices to reach the stage of vast production.

1.8 Objectives of the Present Study

The aim of the present study is to design and fabricate a miniature thermoacoustic cooler to produce sufficient cooling power to cool electric boards for future coupling.

The most important challenges to face during this project can be as follow:

- Designing a traveling-wave thermoacoustic refrigerator driven by an ordinary loudspeaker.

- The overall dimensions of the constructed refrigerator should be relatively small to enable the potential of coupling with electrical/electronic boards for thermal management.
- Achieving certain acoustic conditions of the ordinary loudspeaker by altering the phase difference between the oscillating velocity (volume flow rate) and pressure together with the appropriate acoustic impedance to reach the optimum performance in terms of electrical to acoustic powers conversion.
- Reducing acoustic power losses within the resonator to increase the overall efficiency of the designed thermoacoustic refrigerator.
- Finally, keeping the total cost of the fabricated thermoacoustic cooler as minimum as possible.

1.9 Outline of Thesis

The thesis consists of six chapters and three appendices.

Chapter One: presents a brief description of the background of thermoacoustic, the motivations for research and the aims and objectives of the current study.

Chapter Two: introduces and reviews the practical configurations of thermoacoustic devices.

Chapter Three: firstly, the main focus in this chapter is on the performance and analysis of the given acoustic driver available for this project. In addition, it describes a preliminary design of a thermoacoustic looped-tube cooler, and studies the effect of the parameters of each component of the cooler on acoustic conditions. It then provides an optimum (theoretically) design for thermoacoustic cooler. Finally, it provides the actual design of the cooler.

Chapter Four: It describes the construction of the experimental device and its components in addition to the instrumentation used.

Chapter Five: Shows the experimental results and discusses them. Firstly, the results of the preliminary experiments regarding the optimum operating points of the experimental device are shown and discussed. The effects of the applied cooling load, operating frequency and mean pressure on the performances of thermoacoustic cooler have been also presented and discussed in this chapter.

Chapter Six: presents the conclusions and recommended based on the findings of this research.